

## Supporting Information

### D-π-A type conjugated indanedione derivatives: Ultrafast broadband nonlinear absorption responses and transient dynamics

Lu Chen<sup>a</sup>, Xingzhi Wu \*<sup>b</sup>, Zhongguo Li<sup>c</sup>, Ruipeng Niu<sup>d</sup>, Wenfa Zhou<sup>d</sup>, Kun Liu<sup>a</sup>, Yingfei Sun<sup>a</sup>, Zhangyang Shao<sup>a</sup>, Junyi Yang \*<sup>a</sup> and Yinglin Song \*<sup>a,d</sup>

*a.* School of Physical Science and Technology, Soochow University, Suzhou 215006, People's Republic of China.

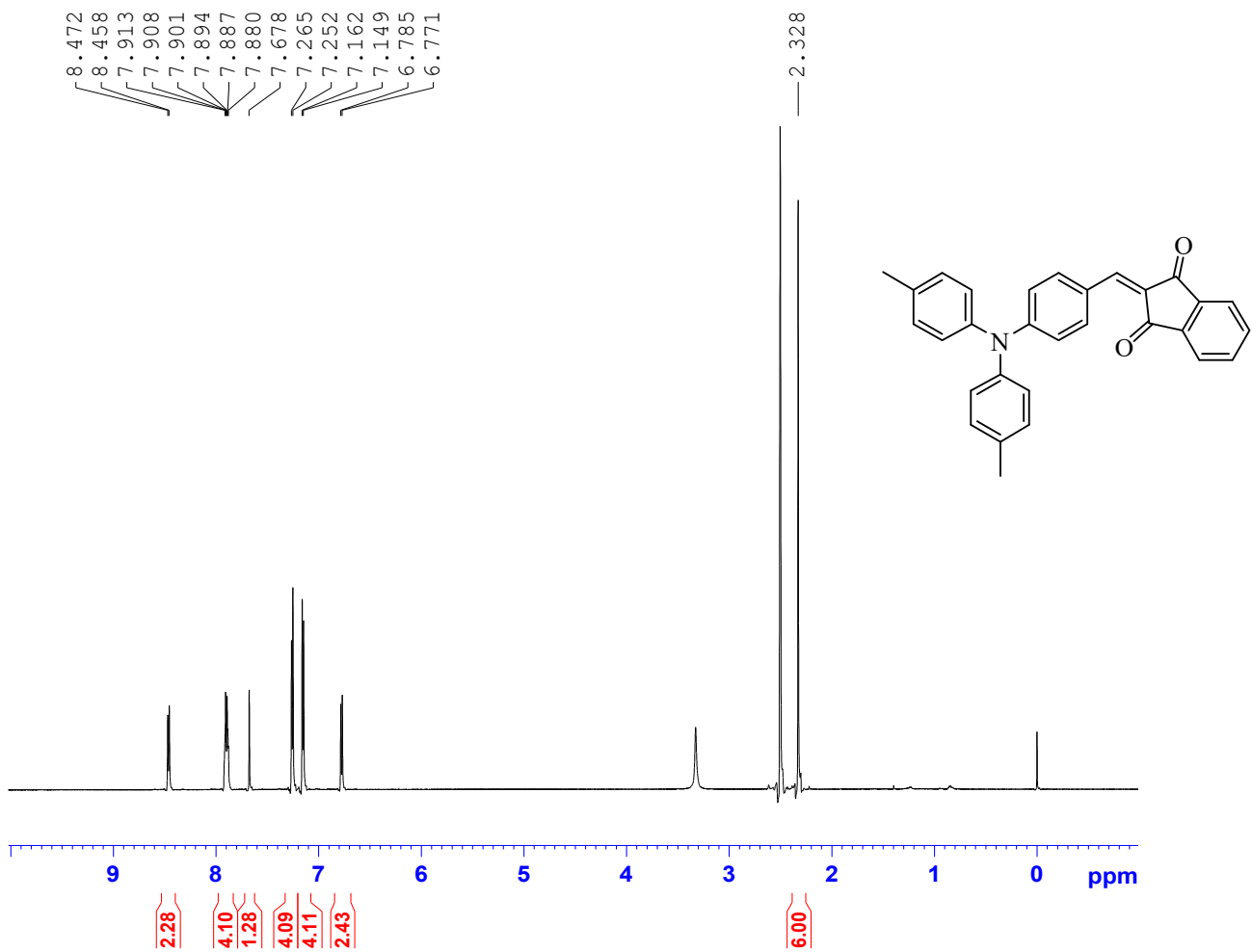
*b.* School of Physical Science and Technology, Suzhou University of Science and Technology, Suzhou University of Science and Technology, Suzhou 215009, People's Republic of China.

*c.* School of Electronic and Information Engineering, Changshu Institute of Technology, Changshu 215500, China.

*d.* Department of Physics, Harbin Institute of Technology, Harbin 150001, People's Republic of China.

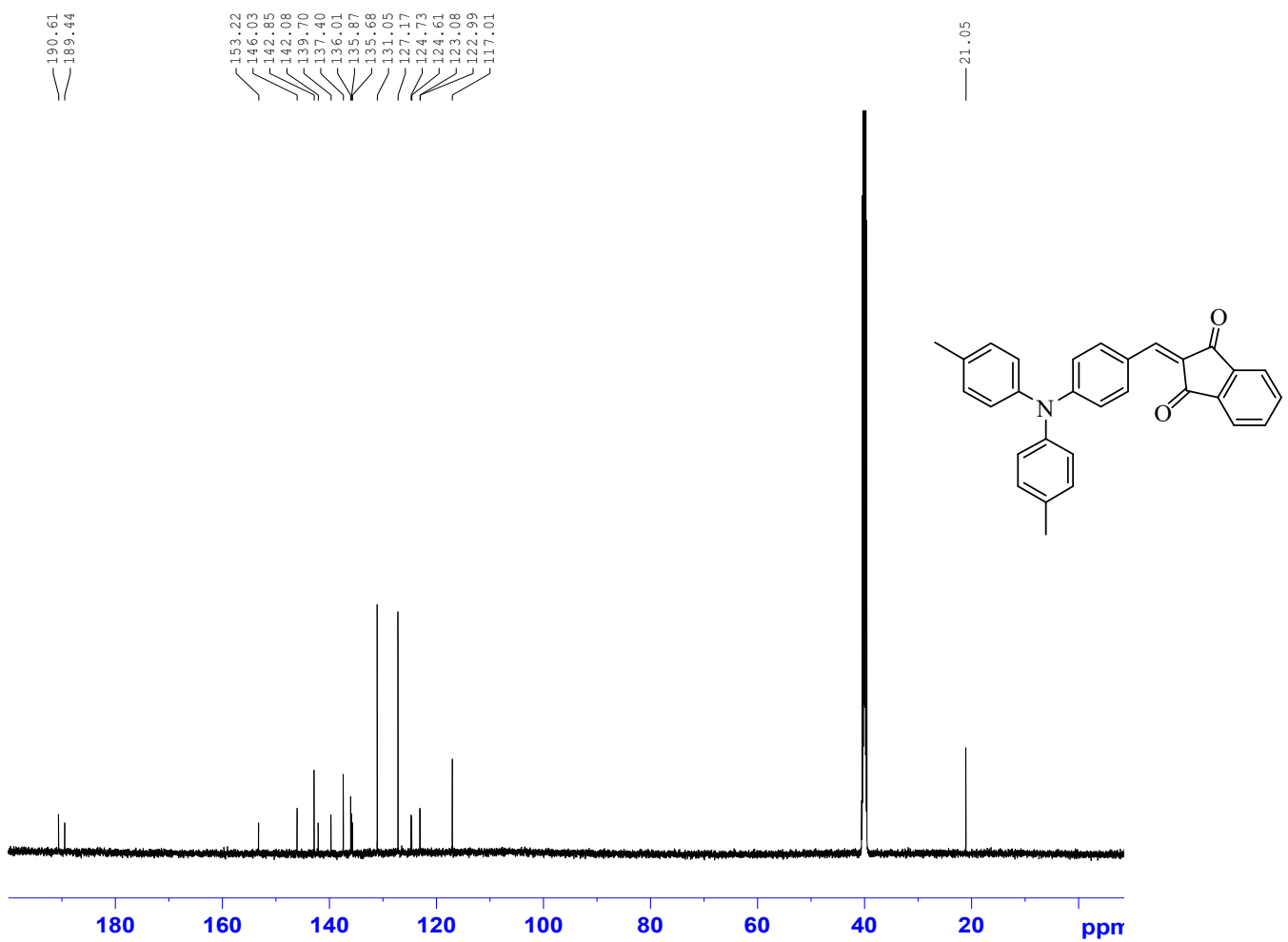
\* Corresponding authors:

[wuxingzhi@usts.edu.cn](mailto:wuxingzhi@usts.edu.cn), [yjy2010@suda.edu.cn](mailto:yjy2010@suda.edu.cn), and [ylsong@hit.edu.cn](mailto:ylsong@hit.edu.cn)



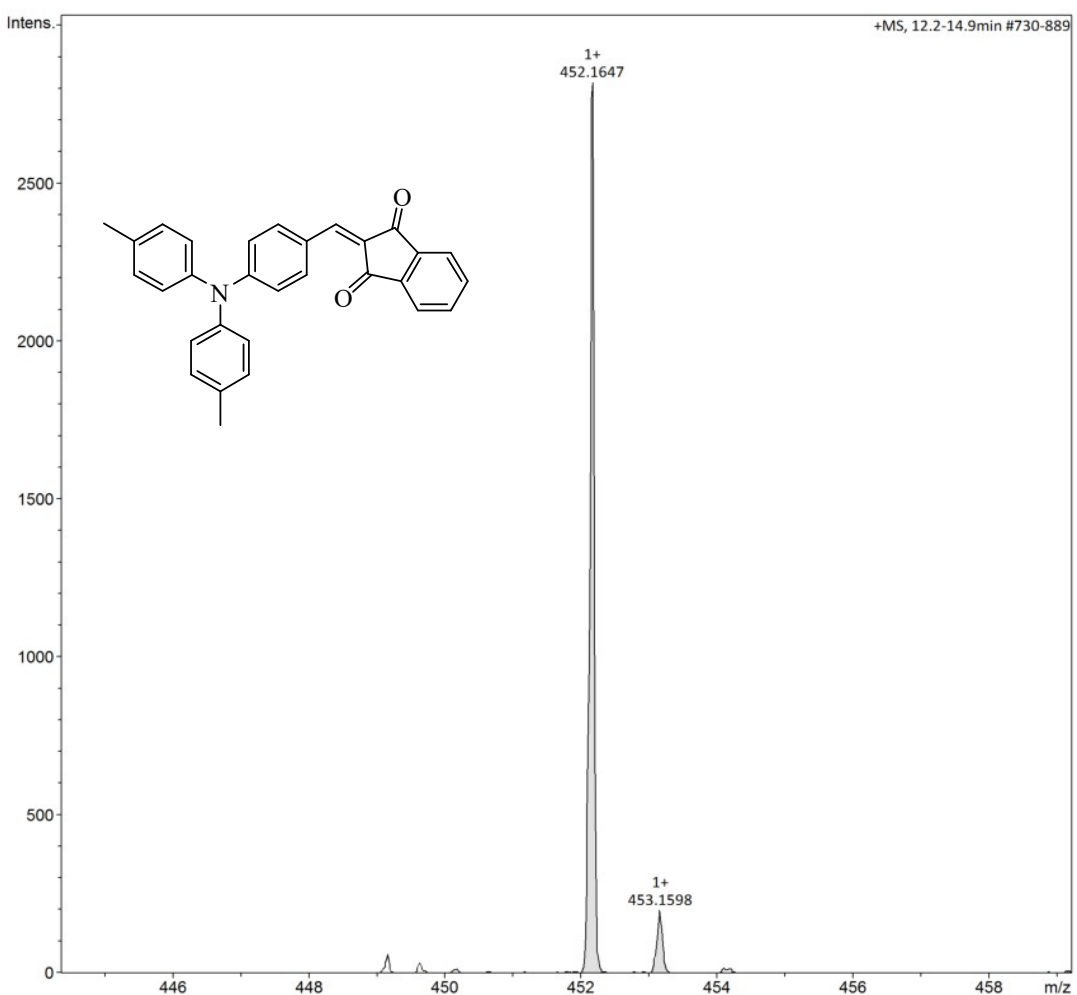
<sup>1</sup>H NMR  $\delta$ /ppm (600 MHz, DMSO) : 8.472~8.458 (d, 2H,  $J=8.4$  Hz) , 7.913~7.880 (m, 4H) , 7.678 (s, 1H) , 7.265~7.252 (d, 4H,  $J=7.8$ Hz) , 7.162~7.149 (d, 4H,  $J=7.8$  Hz) , 6.785~6.771 (d, 2H,  $J=8.4$  Hz) , 2.238 (s, 6H) .

**Figure S1.** <sup>1</sup>H-NMR of INB3.



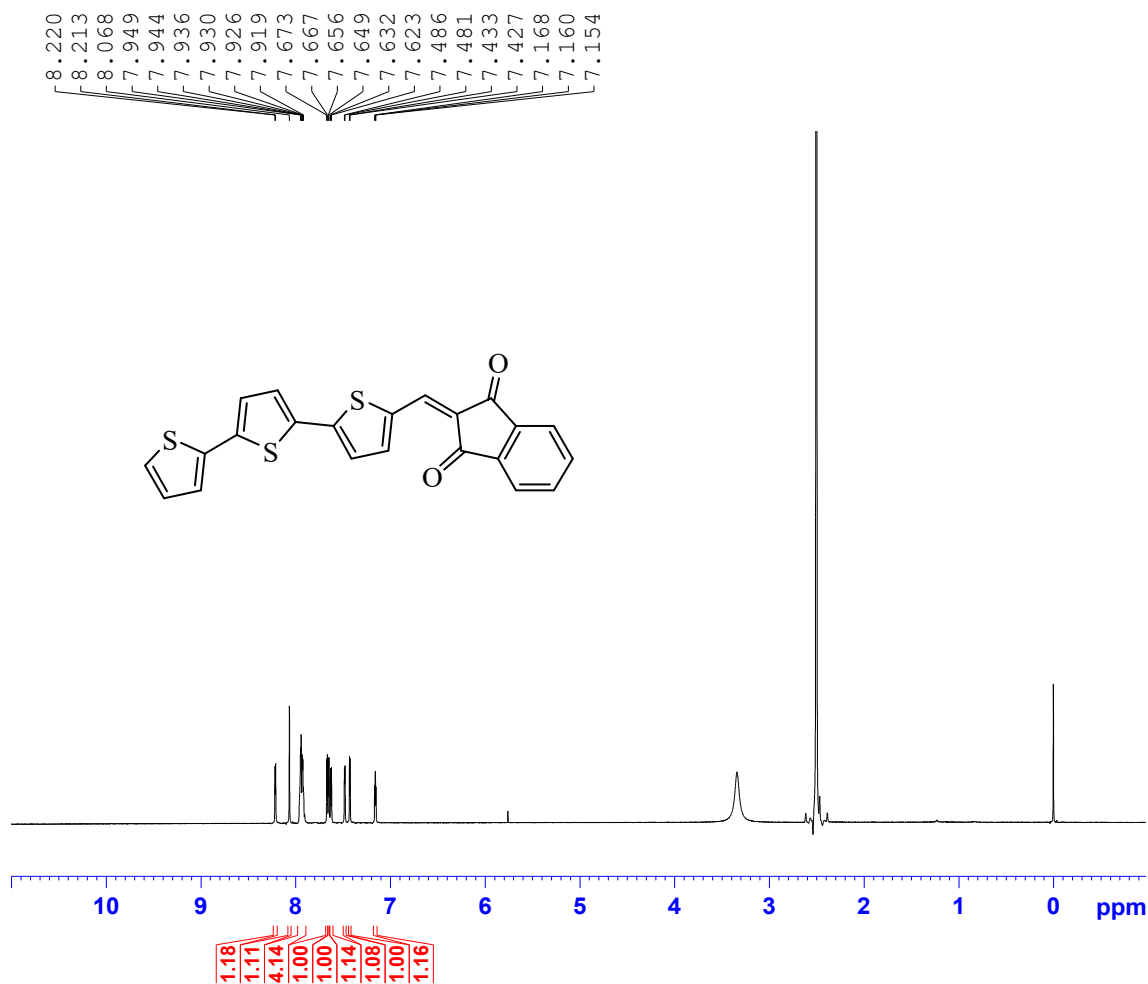
$^{13}\text{C}$  NMR  $\delta$ /ppm (150 MHz, DMSO): 190.61, 189.44, 153.22, 146.03, 142.85, 142.08, 142.00, 139.70, 137.40, 136.01, 135.87, 135.68, 131.05, 127.17, 124.73, 124.61, 123.08, 122.99, 117.01, 21.05.

**Figure S2.**  $^{13}\text{C}$ -NMR of INB3.



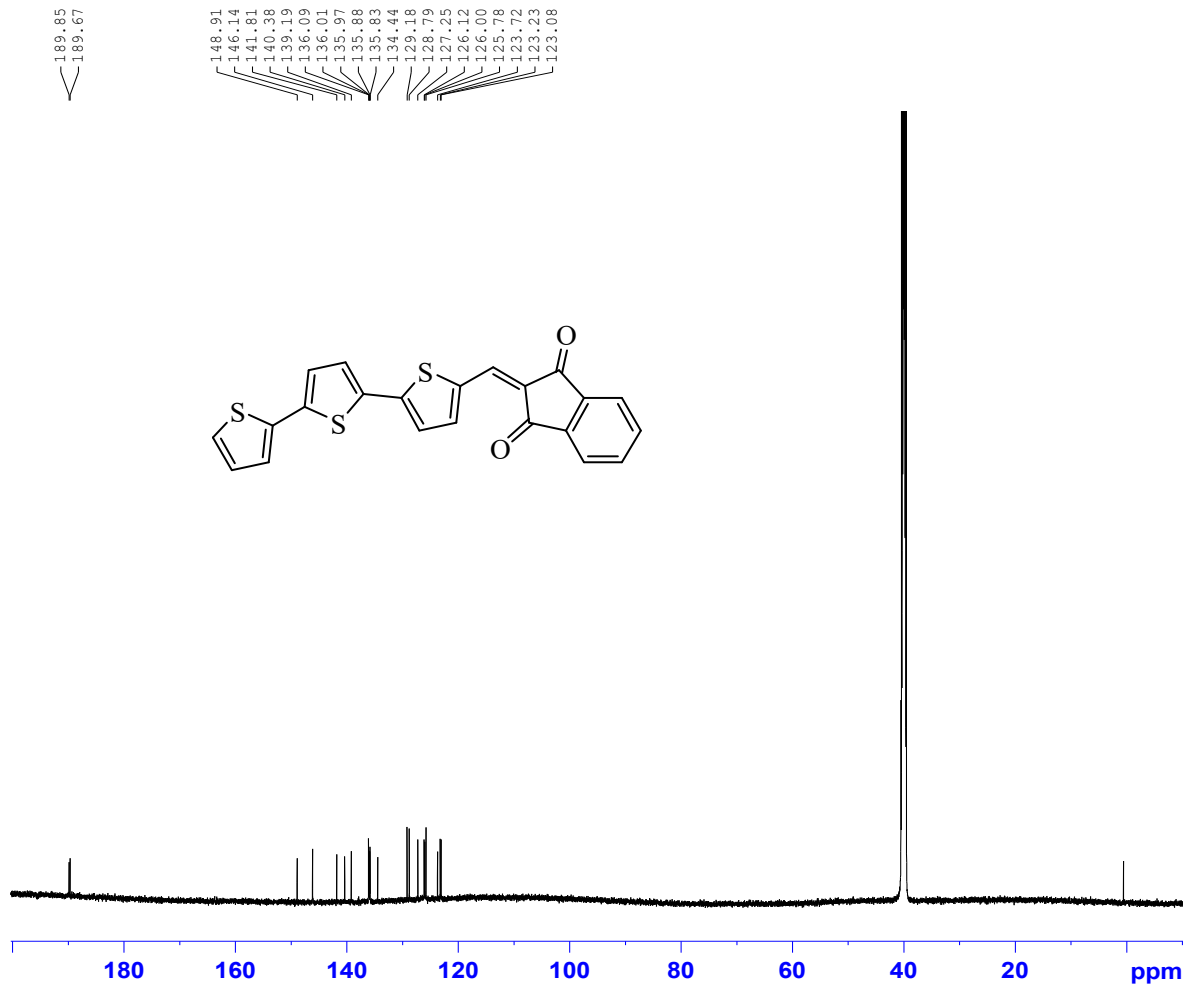
LC-MS<sup>+</sup> (ESI) m/z: found ([M<sup>+</sup> Na<sup>+</sup>]): 452.1647, calc. for (C<sub>30</sub>H<sub>23</sub>O<sub>2</sub>N): 429.52

**Figure S3.** LCMS spectra of INB3.



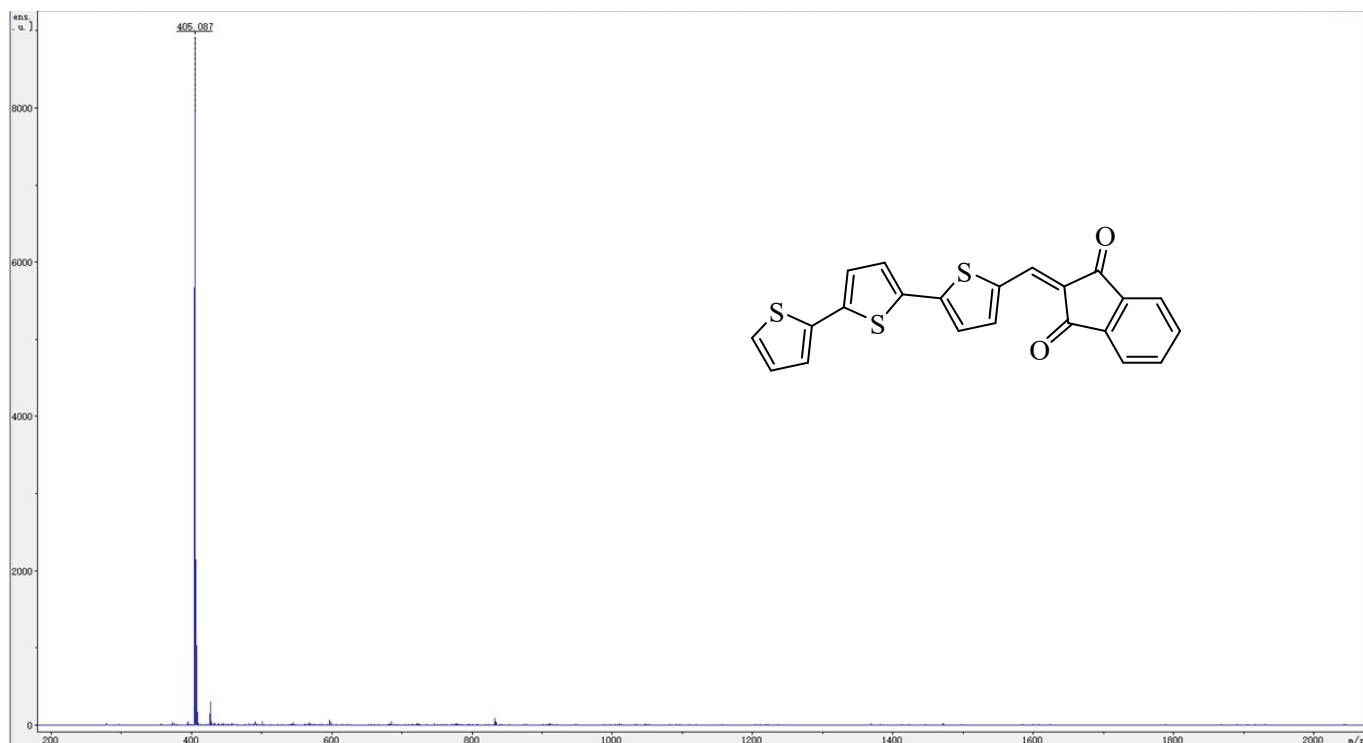
<sup>1</sup>H NMR δ/ppm (600 MHz, DMSO): 8.220~8.213 (d, 1H, J=4.2 Hz), 8.068 (s, 1H), 7.949~7.919 (m, 4H), 6.673~6.667 (d, 1H, J=3.6 Hz), 6.656~6.649 (d, 1H, J=4.2 Hz), 6.632~6.623 (d, 1H, J=5.4 Hz), 7.486~7.481 (d, 1H, J=3.0 Hz), 7.433~7.427 (d, 1H, J=3.6 Hz), 7.168~7.154 (t, 1H, J=4.2 Hz).

**Figure S4.** <sup>1</sup>H-NMR of INT3.



$^{13}\text{C}$  NMR  $\delta/\text{ppm}$  (150 MHz, DMSO): 189.85, 189.67, 148.91, 146.14, 141.81, 140.38, 139.19, 136.09, 136.01, 135.97, 135.88, 135.83, 134.44, 129.18, 128.79, 127.25, 126.12, 26.00, 125.78, 113.72, 123.23, 123.08.

**Figure S5.**  $^{13}\text{C}$ -NMR of INT3.



LC-MS (ESI)  $m/z$ : found ([M+H<sup>+</sup>]): 405.097, calc. for (C<sub>30</sub>H<sub>23</sub>O<sub>2</sub>N): 404.53

**Figure S6.** LCMS spectra of INT3.

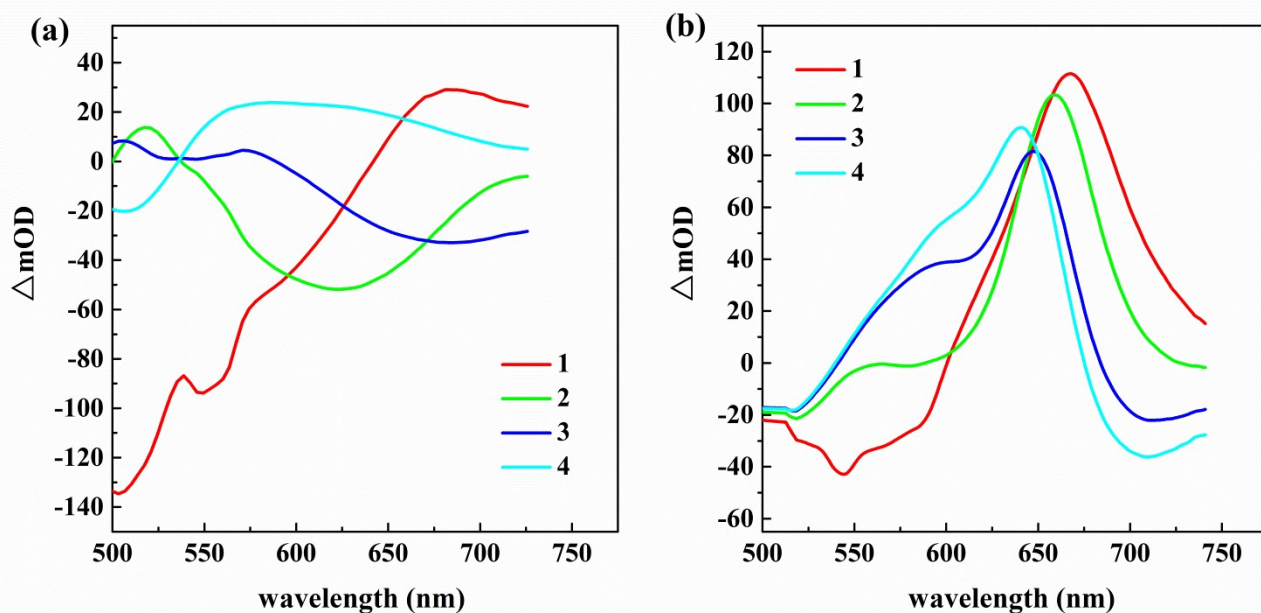


**Figure S7.** Evolution Associated Difference Spectra (EADS) are plotted for INB3 (a) and INT3 (b). Spectral components extracted from global and target analysis, providing information about the evolution of TAS. Four spectral components in total are used and labelled from 1 to 4.

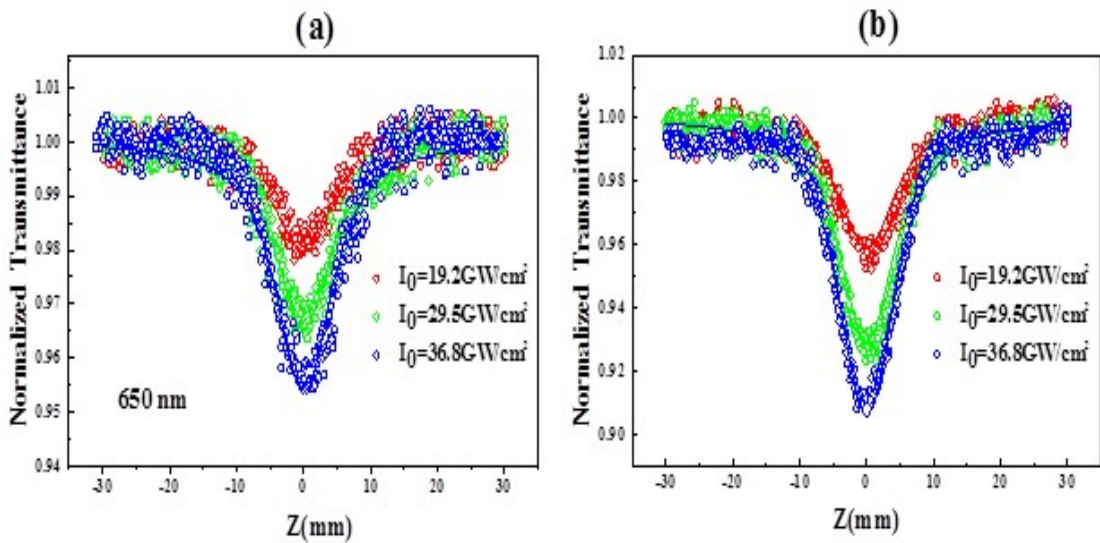


**Figure S8.** (a) and (b) are fs open-aperture Z-scan experiments of INB3 and INT3 at 650 nm, respectively. The open circles are the experimental data and the solid lines represent the numerical fitting.

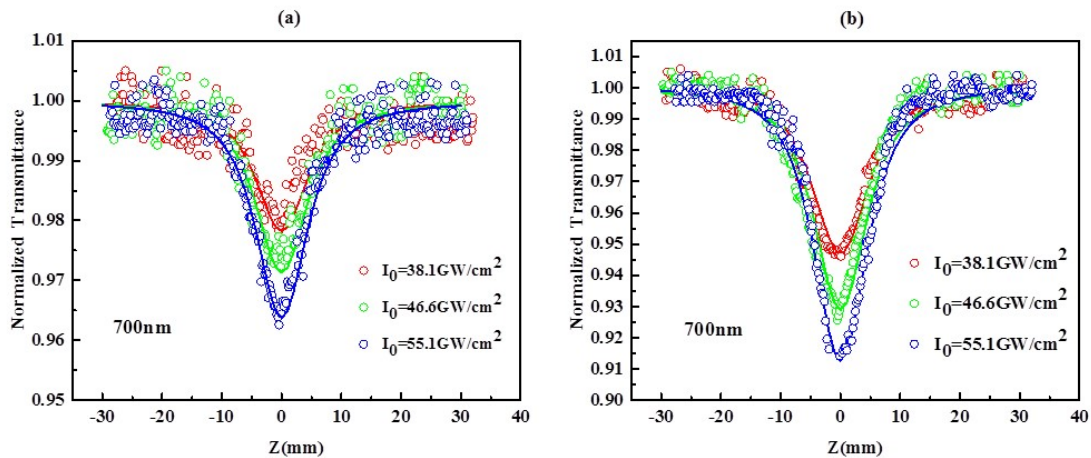


**Figure S9.** (a) and (b) are fs open-aperture Z-scan experiments of INB3 and INT3 at 700 nm, respectively. The open circles are the experimental data and the solid lines represent the numerical fitting.

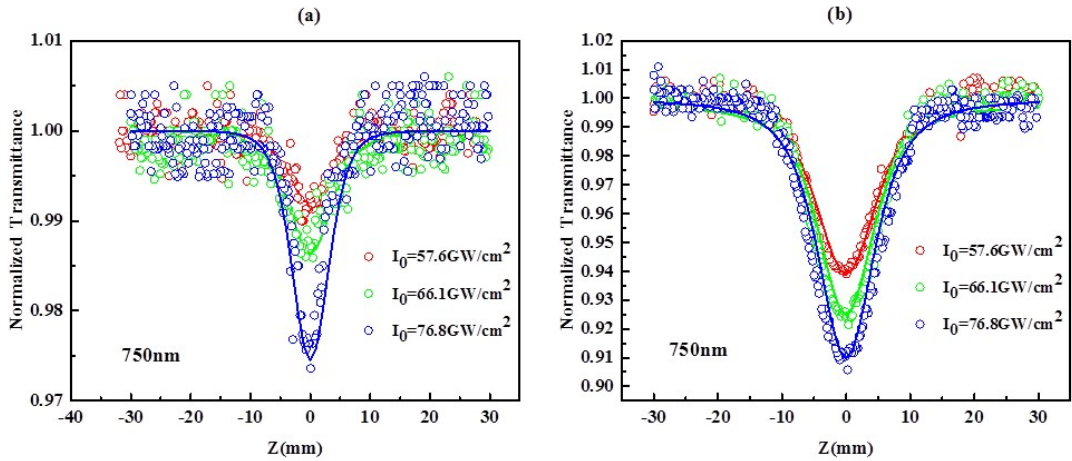


**Figure S10.** (a) and (b) are fs open-aperture Z-scan experiments of INB3 and INT3 at 750 nm, respectively. The open circles are the experimental data and the solid lines represent the numerical fitting.

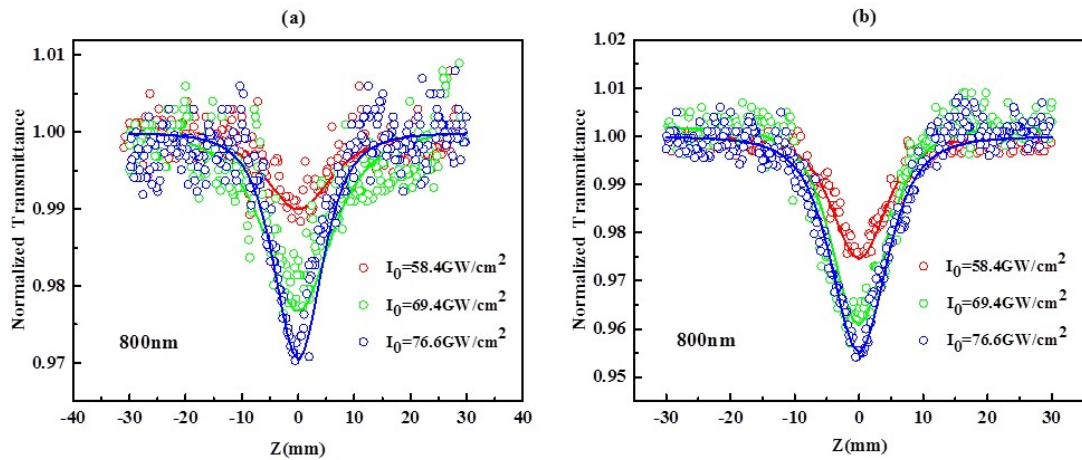


**Figure S11.** (a) and (b) are fs open-aperture Z-scan experiments of INB3 and INT3 at 800 nm, respectively. The open circles are the experimental data and the solid lines represent the numerical fitting.

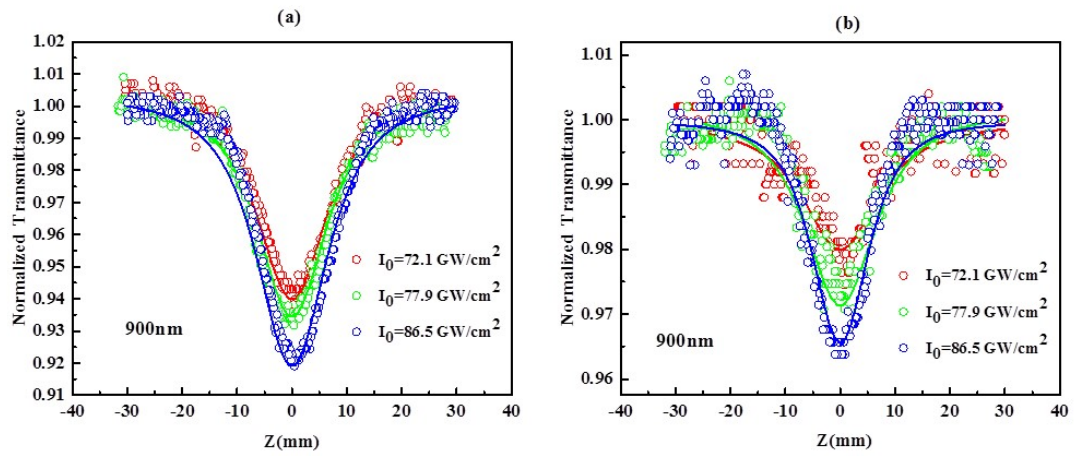


**Figure S12.** (a) and (b) are fs open-aperture Z-scan experiments of INB3 and INT3 at 900 nm, respectively. The open circles are the experimental data and the solid lines represent the numerical fitting.

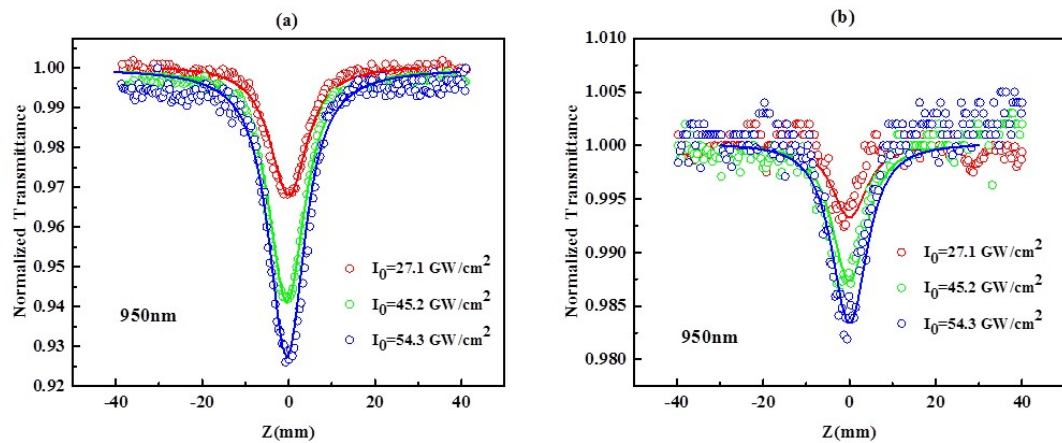


**Figure S13.** (a) and (b) are fs open-aperture Z-scan experiments of INB3 and INT3 at 950 nm, respectively. The open circles are the experimental data and the solid lines represent the numerical fitting.

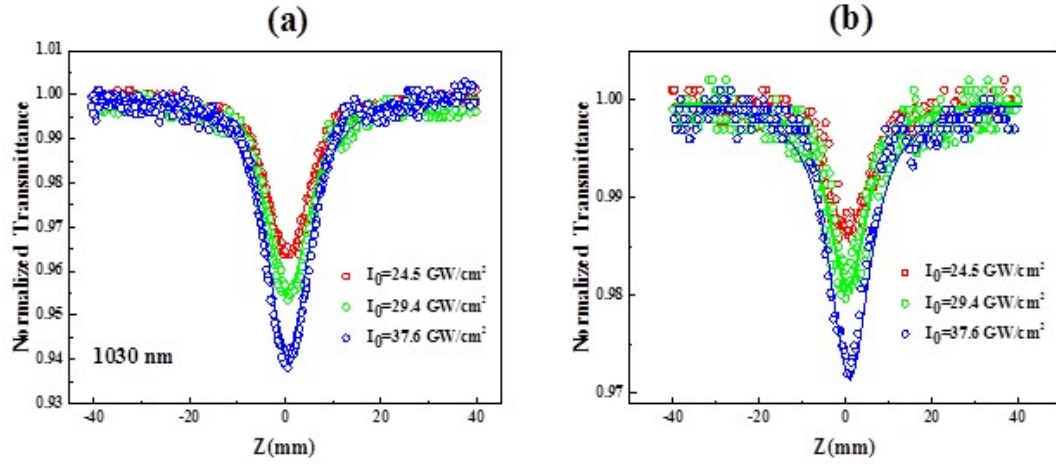


**Figure S14.** (a) and (b) are fs open-aperture Z-scan experiments of INB3 and INT3 at 1030 nm, respectively. The open circles are the experimental data and the solid lines represent the numerical fitting.

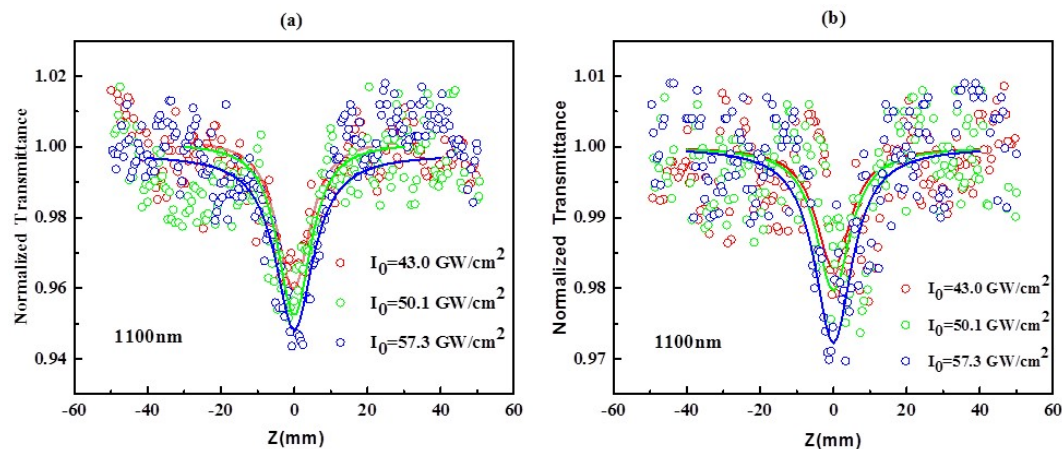


**Figure S15.** (a) and (b) are fs open-aperture Z-scan experiments of INB3 and INT3 at 1100 nm, respectively. The open circles are the experimental data and the solid lines represent the numerical fitting.

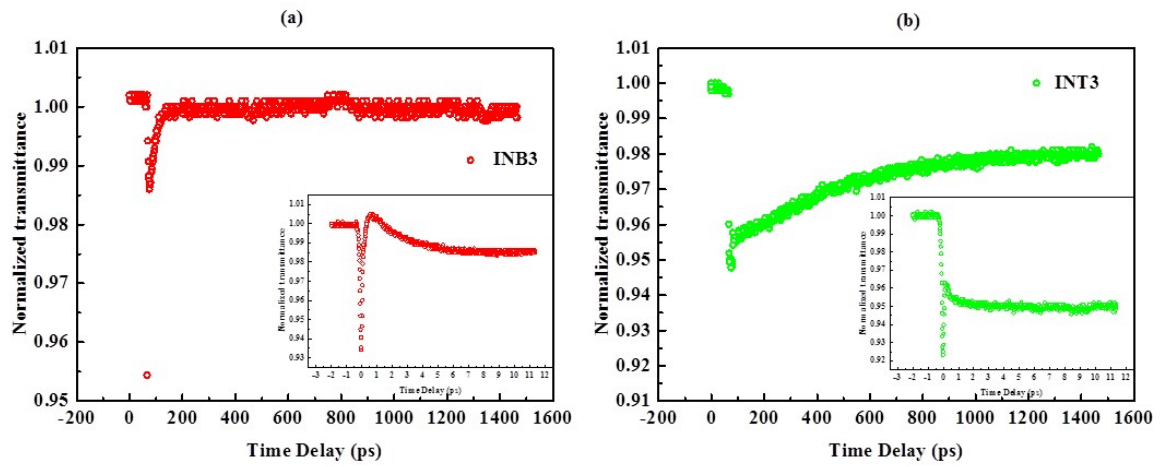


**Figure S16.** (a) and (b) are degenerate pump-probe experiments of INB3 and INT3 at 650 nm, respectively. The dynamic trajectory of nonlinear absorption is plotted and the inset figures show the same short delay dynamics.